

Observation of $\psi(3686) \rightarrow p\bar{p}\phi$

M. Ablikim¹, M. N. Achasov^{10,d}, P. Adlarson⁵⁹, S. Ahmed¹⁵, M. Albrecht⁴, M. Alekseev^{58A,58C},
A. Amoroso^{58A,58C}, F. F. An¹, Q. An^{55,43}, Y. Bai⁴², O. Bakina²⁷, R. Baldini Ferroli^{23A}, Y. Ban³⁵, K. Begzsuren²⁵,
J. V. Bennett⁵, N. Berger²⁶, M. Bertani^{23A}, D. Bettoni^{24A}, F. Bianchi^{58A,58C}, J. Biernat⁵⁹, J. Bloms⁵², I. Boyko²⁷,
R. A. Briere⁵, H. Cai⁶⁰, X. Cai^{1,43}, A. Calcaterra^{23A}, G. F. Cao^{1,47}, N. Cao^{1,47}, S. A. Cetin^{46B}, J. Chai^{58C},
J. F. Chang^{1,43}, W. L. Chang^{1,47}, G. Chelkov^{27,b,c}, D. Y. Chen⁶, G. Chen¹, H. S. Chen^{1,47}, J. C. Chen¹,
M. L. Chen^{1,43}, S. J. Chen³³, Y. B. Chen^{1,43}, W. Cheng^{58C}, G. Cibinetto^{24A}, F. Cossio^{58C}, X. F. Cui³⁴,
H. L. Dai^{1,43}, J. P. Dai^{38,h}, X. C. Dai^{1,47}, A. Dbeyssi¹⁵, D. Dedovich²⁷, Z. Y. Deng¹, A. Denig²⁶, I. Denysenko²⁷,
M. Destefanis^{58A,58C}, F. De Mori^{58A,58C}, Y. Ding³¹, C. Dong³⁴, J. Dong^{1,43}, L. Y. Dong^{1,47}, M. Y. Dong^{1,43,47},
Z. L. Dou³³, S. X. Du⁶³, J. Z. Fan⁴⁵, J. Fang^{1,43}, S. S. Fang^{1,47}, Y. Fang¹, R. Farinelli^{24A,24B}, L. Fava^{58B,58C},
F. Feldbauer⁴, G. Felici^{23A}, C. Q. Feng^{55,43}, M. Fritsch⁴, C. D. Fu¹, Y. Fu¹, Q. Gao¹, X. L. Gao^{55,43}, Y. Gao⁴⁵,
Y. Gao⁵⁶, Y. G. Gao⁶, Z. Gao^{55,43}, B. Garillon²⁶, I. Garzia^{24A}, E. M. Gersabeck⁵⁰, A. Gilman⁵¹, K. Goetzen¹¹,
L. Gong³⁴, W. X. Gong^{1,43}, W. Gradl²⁶, M. Greco^{58A,58C}, L. M. Gu³³, M. H. Gu^{1,43}, S. Gu², Y. T. Gu¹³,
A. Q. Guo²², L. B. Guo³², R. P. Guo³⁶, Y. P. Guo²⁶, A. Guskov²⁷, S. Han⁶⁰, X. Q. Hao¹⁶, F. A. Harris⁴⁸,
K. L. He^{1,47}, F. H. Heinsius⁴, T. Held⁴, Y. K. Heng^{1,43,47}, Y. R. Hou⁴⁷, Z. L. Hou¹, H. M. Hu^{1,47}, J. F. Hu^{38,h},
T. Hu^{1,43,47}, Y. Hu¹, G. S. Huang^{55,43}, J. S. Huang¹⁶, X. T. Huang³⁷, X. Z. Huang³³, Z. L. Huang³¹, N. Huesken⁵²,
T. Hussain⁵⁷, W. Ikegami Andersson⁵⁹, W. Imoehl²², M. Irshad^{55,43}, Q. Ji¹, Q. P. Ji¹⁶, X. B. Ji^{1,47}, X. L. Ji^{1,43},
H. L. Jiang³⁷, X. S. Jiang^{1,43,47}, X. Y. Jiang³⁴, J. B. Jiao³⁷, Z. Jiao¹⁸, D. P. Jin^{1,43,47}, S. Jin³³, Y. Jin⁴⁹,
T. Johansson⁵⁹, N. Kalantar-Nayestanaki²⁹, X. S. Kang³¹, R. Kappert²⁹, M. Kavatsyuk²⁹, B. C. Ke¹, I. K. Keshk⁴,
T. Khan^{55,43}, A. Khoukaz⁵², P. Kiese²⁶, R. Kiuchi¹, R. Kliemt¹¹, L. Koch²⁸, O. B. Kolcu^{46B,f}, B. Kopf⁴,
M. Kuemmel⁴, M. Kuessner⁴, A. Kupsc⁵⁹, M. Kurth¹, M. G. Kurth^{1,47}, W. Kühn²⁸, J. S. Lange²⁸, P. Larin¹⁵,
L. Lavezzi^{58C}, H. Leithoff²⁶, T. Lenz²⁶, C. Li⁵⁹, Cheng Li^{55,43}, D. M. Li⁶³, F. Li^{1,43}, F. Y. Li³⁵, G. Li¹, H. B. Li^{1,47},
H. J. Li^{9,j}, J. C. Li¹, J. W. Li⁴¹, Ke Li¹, L. K. Li¹, Lei Li³, P. L. Li^{55,43}, P. R. Li³⁰, Q. Y. Li³⁷, W. D. Li^{1,47},
W. G. Li¹, X. H. Li^{55,43}, X. L. Li³⁷, X. N. Li^{1,43}, X. Q. Li³⁴, Z. B. Li⁴⁴, Z. Y. Li⁴⁴, H. Liang^{1,47}, H. Liang^{55,43},
Y. F. Liang⁴⁰, Y. T. Liang²⁸, G. R. Liao¹², L. Z. Liao^{1,47}, J. Libby²¹, C. X. Lin⁴⁴, D. X. Lin¹⁵, Y. J. Lin¹³,
B. Liu^{38,h}, B. J. Liu¹, C. X. Liu¹, D. Liu^{55,43}, D. Y. Liu^{38,h}, F. H. Liu³⁹, Fang Liu¹, Feng Liu⁶, H. B. Liu¹³,
H. M. Liu^{1,47}, Huanhuan Liu¹, Huihui Liu¹⁷, J. B. Liu^{55,43}, J. Y. Liu^{1,47}, K. Y. Liu³¹, Ke Liu⁶, Q. Liu⁴⁷,
S. B. Liu^{55,43}, T. Liu^{1,47}, X. Liu³⁰, X. Y. Liu^{1,47}, Y. B. Liu³⁴, Z. A. Liu^{1,43,47}, Zhiqing Liu²⁶, Y. F. Long³⁵,
X. C. Lou^{1,43,47}, H. J. Lu¹⁸, J. D. Lu^{1,47}, J. G. Lu^{1,43}, Y. Lu¹, Y. P. Lu^{1,43}, C. L. Luo³², M. X. Luo⁶², P. W. Luo⁴⁴,
T. Luo^{9,j}, X. L. Luo^{1,43}, S. Lusso^{58C}, X. R. Lyu⁴⁷, F. C. Ma³¹, H. L. Ma¹, L. L. Ma³⁷, M. M. Ma^{1,47}, Q. M. Ma¹,
X. N. Ma³⁴, X. X. Ma^{1,47}, X. Y. Ma^{1,43}, Y. M. Ma³⁷, F. E. Maas¹⁵, M. Maggiora^{58A,58C}, S. Maldaner²⁶, S. Malde⁵³,
Q. A. Malik⁵⁷, A. Mangoni^{23B}, Y. J. Mao³⁵, Z. P. Mao¹, S. Marcello^{58A,58C}, Z. X. Meng⁴⁹, J. G. Messchendorp²⁹,
G. Mezzadri^{24A}, J. Min^{1,43}, T. J. Min³³, R. E. Mitchell²², X. H. Mo^{1,43,47}, Y. J. Mo⁶, C. Morales Morales¹⁵,
N. Yu. Muchnoi^{10,d}, H. Muramatsu⁵¹, A. Mustafa⁴, S. Nakhoul^{11,g}, Y. Nefedov²⁷, F. Nerling^{11,g}, I. B. Nikolaev^{10,d},
Z. Ning^{1,43}, S. Nisar^{8,k}, S. L. Niu^{1,43}, S. L. Olsen⁴⁷, Q. Ouyang^{1,43,47}, S. Pacetti^{23B}, Y. Pan^{55,43}, M. Papenbrock⁵⁹,
P. Patteri^{23A}, M. Pelizzaeus⁴, H. P. Peng^{55,43}, K. Peters^{11,g}, J. Pettersson⁵⁹, J. L. Ping³², R. G. Ping^{1,47},
A. Pitka⁴, R. Poling⁵¹, V. Prasad^{55,43}, M. Qi³³, T. Y. Qi², S. Qian^{1,43}, C. F. Qiao⁴⁷, N. Qin⁶⁰, X. P. Qin¹³,
X. S. Qin⁴, Z. H. Qin^{1,43}, J. F. Qiu¹, S. Q. Qu³⁴, K. H. Rashid^{57,i}, C. F. Redmer²⁶, M. Richter⁴, M. Ripka²⁶,
A. Rivetti^{58C}, V. Rodin²⁹, M. Rolo^{58C}, G. Rong^{1,47}, Ch. Rosner¹⁵, M. Rump⁵², A. Sarantsev^{27,e}, M. Savrié^{24B},
K. Schoenning⁵⁹, W. Shan¹⁹, X. Y. Shan^{55,43}, M. Shao^{55,43}, C. P. Shen², P. X. Shen³⁴, X. Y. Shen^{1,47},
H. Y. Sheng¹, X. Shi^{1,43}, X. D. Shi^{55,43}, J. J. Song³⁷, Q. Q. Song^{55,43}, X. Y. Song¹, S. Sosio^{58A,58C}, C. Sowa⁴,
S. Spataro^{58A,58C}, F. F. Sui³⁷, G. X. Sun¹, J. F. Sun¹⁶, L. Sun⁶⁰, S. S. Sun^{1,47}, X. H. Sun¹, Y. J. Sun^{55,43},
Y. K. Sun^{55,43}, Y. Z. Sun¹, Z. J. Sun^{1,43}, Z. T. Sun¹, Y. T. Tan^{55,43}, C. J. Tang⁴⁰, G. Y. Tang¹, X. Tang¹,
V. Thoren⁵⁹, B. Tsednee²⁵, I. Uman^{46D}, B. Wang¹, B. L. Wang⁴⁷, C. W. Wang³³, D. Y. Wang³⁵, H. H. Wang³⁷,
K. Wang^{1,43}, L. L. Wang¹, L. S. Wang¹, M. Wang³⁷, M. Z. Wang³⁵, Meng Wang^{1,47}, P. L. Wang¹, R. M. Wang⁶¹,
W. P. Wang^{55,43}, X. Wang³⁵, X. F. Wang¹, X. L. Wang^{9,j}, Y. Wang^{55,43}, Y. Wang⁴⁴, Y. F. Wang^{1,43,47},
Z. Wang^{1,43}, Z. G. Wang^{1,43}, Z. Y. Wang¹, Zongyuan Wang^{1,47}, T. Weber⁴, D. H. Wei¹², P. Weidenkaff²⁶,
H. W. Wen³², S. P. Wen¹, U. Wiedner⁴, G. Wilkinson⁵³, M. Wolke⁵⁹, L. H. Wu¹, L. J. Wu^{1,47}, Z. Wu^{1,43},
L. Xia^{55,43}, Y. Xia²⁰, S. Y. Xiao¹, Y. J. Xiao^{1,47}, Z. J. Xiao³², Y. G. Xie^{1,43}, Y. H. Xie⁶, T. Y. Xing^{1,47},
X. A. Xiong^{1,47}, Q. L. Xiu^{1,43}, G. F. Xu¹, L. Xu¹, Q. J. Xu¹⁴, W. Xu^{1,47}, X. P. Xu⁴¹, F. Yan⁵⁶, L. Yan^{58A,58C},
W. B. Yan^{55,43}, W. C. Yan², Y. H. Yan²⁰, H. J. Yang^{38,h}, H. X. Yang¹, L. Yang⁶⁰, R. X. Yang^{55,43}, S. L. Yang^{1,47},
Y. H. Yang³³, Y. X. Yang¹², Yifan Yang^{1,47}, Z. Q. Yang²⁰, M. Ye^{1,43}, M. H. Ye⁷, J. H. Yin¹, Z. Y. You⁴⁴,
B. X. Yu^{1,43,47}, C. X. Yu³⁴, J. S. Yu²⁰, C. Z. Yuan^{1,47}, X. Q. Yuan³⁵, Y. Yuan¹, A. Yuncu^{46B,a}, A. A. Zafar⁵⁷,

Y. Zeng²⁰, B. X. Zhang¹, B. Y. Zhang^{1,43}, C. C. Zhang¹, D. H. Zhang¹, H. H. Zhang⁴⁴, H. Y. Zhang^{1,43}, J. Zhang^{1,47}, J. L. Zhang⁶¹, J. Q. Zhang⁴, J. W. Zhang^{1,43,47}, J. Y. Zhang¹, J. Z. Zhang^{1,47}, K. Zhang^{1,47}, L. Zhang⁴⁵, S. F. Zhang³³, T. J. Zhang^{38,h}, X. Y. Zhang³⁷, Y. Zhang^{55,43}, Y. H. Zhang^{1,43}, Y. T. Zhang^{55,43}, Yang Zhang¹, Yao Zhang¹, Yi Zhang^{9,j}, Yu Zhang⁴⁷, Z. H. Zhang⁶, Z. P. Zhang⁵⁵, Z. Y. Zhang⁶⁰, G. Zhao¹, J. W. Zhao^{1,43}, J. Y. Zhao^{1,47}, J. Z. Zhao^{1,43}, Lei Zhao^{55,43}, Ling Zhao¹, M. G. Zhao³⁴, Q. Zhao¹, S. J. Zhao⁶³, T. C. Zhao¹, Y. B. Zhao^{1,43}, Z. G. Zhao^{55,43}, A. Zhemchugov^{27,b}, B. Zheng⁵⁶, J. P. Zheng^{1,43}, Y. Zheng³⁵, Y. H. Zheng⁴⁷, B. Zhong³², L. Zhou^{1,43}, L. P. Zhou^{1,47}, Q. Zhou^{1,47}, X. Zhou⁶⁰, X. K. Zhou⁴⁷, X. R. Zhou^{55,43}, Xiaoyu Zhou²⁰, Xu Zhou²⁰, A. N. Zhu^{1,47}, J. Zhu³⁴, J. Zhu⁴⁴, K. Zhu¹, K. J. Zhu^{1,43,47}, S. H. Zhu⁵⁴, W. J. Zhu³⁴, X. L. Zhu⁴⁵, Y. C. Zhu^{55,43}, Y. S. Zhu^{1,47}, Z. A. Zhu^{1,47}, J. Zhuang^{1,43}, B. S. Zou¹, J. H. Zou¹

(BESIII Collaboration)

¹ *Institute of High Energy Physics, Beijing 100049, People's Republic of China*

² *Beihang University, Beijing 100191, People's Republic of China*

³ *Beijing Institute of Petrochemical Technology, Beijing 102617, People's Republic of China*

⁴ *Bochum Ruhr-University, D-44780 Bochum, Germany*

⁵ *Carnegie Mellon University, Pittsburgh, Pennsylvania 15213, USA*

⁶ *Central China Normal University, Wuhan 430079, People's Republic of China*

⁷ *China Center of Advanced Science and Technology, Beijing 100190, People's Republic of China*

⁸ *COMSATS University Islamabad, Lahore Campus, Defence Road, Off Raiwind Road, 54000 Lahore, Pakistan*

⁹ *Fudan University, Shanghai 200443, People's Republic of China*

¹⁰ *G.I. Budker Institute of Nuclear Physics SB RAS (BINP), Novosibirsk 630090, Russia*

¹¹ *GSI Helmholtzcentre for Heavy Ion Research GmbH, D-64291 Darmstadt, Germany*

¹² *Guangxi Normal University, Guilin 541004, People's Republic of China*

¹³ *Guangxi University, Nanning 530004, People's Republic of China*

¹⁴ *Hangzhou Normal University, Hangzhou 310036, People's Republic of China*

¹⁵ *Helmholtz Institute Mainz, Johann-Joachim-Becher-Weg 45, D-55099 Mainz, Germany*

¹⁶ *Henan Normal University, Xinxiang 453007, People's Republic of China*

¹⁷ *Henan University of Science and Technology, Luoyang 471003, People's Republic of China*

¹⁸ *Huangshan College, Huangshan 245000, People's Republic of China*

¹⁹ *Hunan Normal University, Changsha 410081, People's Republic of China*

²⁰ *Hunan University, Changsha 410082, People's Republic of China*

²¹ *Indian Institute of Technology Madras, Chennai 600036, India*

²² *Indiana University, Bloomington, Indiana 47405, USA*

²³ *(A)INFN Laboratori Nazionali di Frascati, I-00044, Frascati, Italy; (B)INFN and University of Perugia, I-06100, Perugia, Italy*

²⁴ *(A)INFN Sezione di Ferrara, I-44122, Ferrara, Italy; (B)University of Ferrara, I-44122, Ferrara, Italy*

²⁵ *Institute of Physics and Technology, Peace Ave. 54B, Ulaanbaatar 13330, Mongolia*

²⁶ *Johannes Gutenberg University of Mainz, Johann-Joachim-Becher-Weg 45, D-55099 Mainz, Germany*

²⁷ *Joint Institute for Nuclear Research, 141980 Dubna, Moscow region, Russia*

²⁸ *Justus-Liebig-Universitaet Giessen, II. Physikalisches Institut, Heinrich-Buff-Ring 16, D-35392 Giessen, Germany*

²⁹ *KVI-CART, University of Groningen, NL-9747 AA Groningen, The Netherlands*

³⁰ *Lanzhou University, Lanzhou 730000, People's Republic of China*

³¹ *Liaoning University, Shenyang 110036, People's Republic of China*

³² *Nanjing Normal University, Nanjing 210023, People's Republic of China*

³³ *Nanjing University, Nanjing 210093, People's Republic of China*

³⁴ *Nankai University, Tianjin 300071, People's Republic of China*

³⁵ *Peking University, Beijing 100871, People's Republic of China*

³⁶ *Shandong Normal University, Jinan 250014, People's Republic of China*

³⁷ *Shandong University, Jinan 250100, People's Republic of China*

³⁸ *Shanghai Jiao Tong University, Shanghai 200240, People's Republic of China*

³⁹ *Shanxi University, Taiyuan 030006, People's Republic of China*

⁴⁰ *Sichuan University, Chengdu 610064, People's Republic of China*

⁴¹ *Soochow University, Suzhou 215006, People's Republic of China*

⁴² *Southeast University, Nanjing 211100, People's Republic of China*

- ⁴³ *State Key Laboratory of Particle Detection and Electronics, Beijing 100049, Hefei 230026, People's Republic of China*
- ⁴⁴ *Sun Yat-Sen University, Guangzhou 510275, People's Republic of China*
- ⁴⁵ *Tsinghua University, Beijing 100084, People's Republic of China*
- ⁴⁶ (A) *Ankara University, 06100 Tandogan, Ankara, Turkey; (B) Istanbul Bilgi University, 34060 Eyup, Istanbul, Turkey; (C) Uludag University, 16059 Bursa, Turkey; (D) Near East University, Nicosia, North Cyprus, Mersin 10, Turkey*
- ⁴⁷ *University of Chinese Academy of Sciences, Beijing 100049, People's Republic of China*
- ⁴⁸ *University of Hawaii, Honolulu, Hawaii 96822, USA*
- ⁴⁹ *University of Jinan, Jinan 250022, People's Republic of China*
- ⁵⁰ *University of Manchester, Oxford Road, Manchester, M13 9PL, United Kingdom*
- ⁵¹ *University of Minnesota, Minneapolis, Minnesota 55455, USA*
- ⁵² *University of Muenster, Wilhelm-Klemm-Str. 9, 48149 Muenster, Germany*
- ⁵³ *University of Oxford, Keble Rd, Oxford, UK OX13RH*
- ⁵⁴ *University of Science and Technology Liaoning, Anshan 114051, People's Republic of China*
- ⁵⁵ *University of Science and Technology of China, Hefei 230026, People's Republic of China*
- ⁵⁶ *University of South China, Hengyang 421001, People's Republic of China*
- ⁵⁷ *University of the Punjab, Lahore-54590, Pakistan*
- ⁵⁸ (A) *University of Turin, I-10125, Turin, Italy; (B) University of Eastern Piedmont, I-15121, Alessandria, Italy; (C) INFN, I-10125, Turin, Italy*
- ⁵⁹ *Uppsala University, Box 516, SE-75120 Uppsala, Sweden*
- ⁶⁰ *Wuhan University, Wuhan 430072, People's Republic of China*
- ⁶¹ *Xinyang Normal University, Xinyang 464000, People's Republic of China*
- ⁶² *Zhejiang University, Hangzhou 310027, People's Republic of China*
- ⁶³ *Zhengzhou University, Zhengzhou 450001, People's Republic of China*
- ^a *Also at Bogazici University, 34342 Istanbul, Turkey*
- ^b *Also at the Moscow Institute of Physics and Technology, Moscow 141700, Russia*
- ^c *Also at the Functional Electronics Laboratory, Tomsk State University, Tomsk, 634050, Russia*
- ^d *Also at the Novosibirsk State University, Novosibirsk, 630090, Russia*
- ^e *Also at the NRC "Kurchatov Institute", PNPI, 188300, Gatchina, Russia*
- ^f *Also at Istanbul Arel University, 34295 Istanbul, Turkey*
- ^g *Also at Goethe University Frankfurt, 60323 Frankfurt am Main, Germany*
- ^h *Also at Key Laboratory for Particle Physics, Astrophysics and Cosmology, Ministry of Education; Shanghai Key Laboratory for Particle Physics and Cosmology; Institute of Nuclear and Particle Physics, Shanghai 200240, People's Republic of China*
- ⁱ *Also at Government College Women University, Sialkot - 51310. Punjab, Pakistan.*
- ^j *Also at Key Laboratory of Nuclear Physics and Ion-beam Application (MOE) and Institute of Modern Physics, Fudan University, Shanghai 200443, People's Republic of China*
- ^k *Also at Harvard University, Department of Physics, Cambridge, MA, 02138, USA*

(Dated: July 23, 2019)

Using a data sample of 4.48×10^8 $\psi(3686)$ events collected with the BESIII detector, we present a first observation of $\psi(3686) \rightarrow p\bar{p}\phi$, and we measure its branching fraction to be $[6.06 \pm 0.38(\text{stat.}) \pm 0.48(\text{syst.})] \times 10^{-6}$. In contrast to the earlier discovery of a threshold enhancement in the $p\bar{p}$ -mass spectrum of the channel $J/\psi \rightarrow \gamma p\bar{p}$, denoted as $X(p\bar{p})$, we do not find a similar enhancement in $\psi(3686) \rightarrow p\bar{p}\phi$. An upper limit of 1.82×10^{-7} at the 90% confidence level on the branching fraction of $\psi(3686) \rightarrow X(p\bar{p})\phi \rightarrow p\bar{p}\phi$ is obtained.

PACS numbers: 13.66.Bc, 14.40.Be

I. INTRODUCTION

An intriguing enhancement near the $p\bar{p}$ -mass threshold, referred to as the $X(p\bar{p})$, was discovered by BES in the channel $J/\psi \rightarrow \gamma p\bar{p}$ [1] and subsequently con-

firmed by CLEO [2] and BESIII [3]. A more recent partial-wave amplitude analysis of $J/\psi \rightarrow \gamma p\bar{p}$ [4] supports the existence of the structure and concludes to a spin-parity assignment of $J^{PC} = 0^{-+}$. There is no experimental evidence of such an enhancement in radia-

tive $\Upsilon(1S) \rightarrow \gamma p\bar{p}$ [5] decay nor in the $J/\psi \rightarrow \omega p\bar{p}$ decay [6]. It is tempting to associate this enhancement with the $X(1835)$, a resonance that was recently confirmed by BESIII [7] after it was first observed in $J/\psi \rightarrow \gamma\pi^+\pi^-\eta'$ decay [8]. Whether or not the $p\bar{p}$ -mass threshold enhancement and the $X(1835)$ are related to the same source still needs further study. As a result, lots of theoretical speculations have been proposed to interpret the nature of this structure, including the quasibound nuclear baryonium [9, 10], a multiquark resonance [11] or an effect caused by final-state interaction (FSI) [12, 13] near the proton-antiproton production threshold.

Most recently, BESIII reported the study of $J/\psi \rightarrow p\bar{p}\phi$ [14] and no evidence of a near-threshold enhancement in the $p\bar{p}$ -mass spectrum was found. Moreover, no significant signatures of resonances in the $p\phi$ or $\bar{p}\phi$ mass spectra were observed. For the decay of $\psi(3686) \rightarrow p\bar{p}\phi$, BES reported an upper limit on the branching fraction $\mathcal{B}(\psi(3686) \rightarrow p\bar{p}\phi)$ of 2.6×10^{-5} at the 90% confidence level (C.L.) [15]. The latest measurement came from CLEO [16], who reported an upper limit on the branching fraction $\mathcal{B}(\psi(3686) \rightarrow p\bar{p}\phi)$ of 2.4×10^{-5} at the 90% C.L.. These experimental observations, together with similar results found in different decays, give rise to a discussion on the nature of the threshold effect and stimulate theoretical developments.

In this work, we report on the data analysis of the charmonium decay $\psi(3686) \rightarrow p\bar{p}\phi$. The data have been obtained with the BESIII detector at the BEPCII storage ring at which a total of $(4.481 \pm 0.029) \times 10^8$ $\psi(3686)$ events [17] were produced in electron-positron annihilations. The aim of this work is to search for a near-threshold enhancement in the $p\bar{p}$ -mass spectrum and to search for $p\phi(\bar{p}\phi)$ resonances that might hint to the existence of pentaquarks with hidden strangeness. Moreover, we measured the branching fraction of the process $\psi(3686) \rightarrow p\bar{p}\phi$ which allows us to inspect the ‘12% rule’ proposed in 1975 [18]. The rule is based on perturbative quantum chromodynamics (QCD) calculations, in which the ratio of the branching fractions of $\psi(3686)$ and J/ψ into the same final hadronic state is given by

$$Q = \frac{B_{\psi(3686) \rightarrow h}}{B_{J/\psi \rightarrow h}} = \frac{B_{\psi(3686) \rightarrow l^+l^-}}{B_{J/\psi \rightarrow l^+l^-}} = (12.4 \pm 0.4)\%. \quad (1)$$

II. DETECTOR AND MONTE CARLO SIMULATION

The BESIII detector is a magnetic spectrometer [19] located at the Beijing Electron Positron Collider (BEPCII) [20]. The cylindrical core of the BESIII detector consists of a helium-based multilayer drift chamber (MDC), a plastic scintillator time-of-flight system (TOF), and a CsI(Tl) electromagnetic calorimeter (EMC), which are all enclosed in a superconducting solenoidal magnet providing a 1.0 T magnetic field. The solenoid is supported by an octagonal flux-return yoke

with resistive plate counter muon identifier modules interleaved with steel. The acceptance of charged particles and photons is 93% over 4π solid angle. The charged-particle momentum resolution at 1 GeV/c is 0.5%, and the dE/dx resolution is 6% for the electrons from Bhabha scattering. The EMC measures photon energies with a resolution of 2.5% (5%) at 1 GeV in the barrel (end cap) region. The time resolution of the TOF barrel part is 68 ps, while that of the end cap part is 110 ps.

Simulated samples produced with the GEANT4-based [21] Monte Carlo (MC) package which includes the geometric description of the BESIII detector and the detector response, are used to determine the detection efficiency and to estimate the backgrounds. The simulation includes the beam energy spread and the initial-state radiation (ISR) in the e^+e^- annihilations modelled with the generator KKMC [22]. The inclusive MC sample consists of the production of the $\psi(3686)$ resonance, and the continuum processes incorporated in KKMC. The known decay modes are modelled with EVTGEN [23] using branching fractions taken from the Particle Data Group (PDG) [24], and the remaining unknown decays from the charmonium states with LUNDCHARM [25]. The final-state radiation (FSR) from charged final-state particles is incorporated with the PHOTOS package [26]. The background is studied using a sample of 5.06×10^8 inclusive $\psi(3686)$ MC events. The analysis is performed in the framework of the BESIII offline software system (BOSS) [27] incorporating the detector calibration, event reconstruction and data storage.

III. DATA ANALYSIS

A. Event selection and background analysis

The $\psi(3686) \rightarrow p\bar{p}\phi$ reaction is identified with the ϕ subsequently decaying into K^+K^- resulting in a final state of four charged tracks, namely $p\bar{p}K^+K^-$. The charged tracks must have been detected in the active region of the MDC, corresponding to $|\cos\theta| < 0.93$, where θ is the polar angle of the charged track with respect to the beam direction. Moreover, the tracks are required to pass within ± 10 cm of the interaction point in the beam direction and within ± 1 cm in the plane perpendicular to the beam. Two of the charged tracks are identified as a proton and an antiproton by using combined TOF and dE/dx information. To improve the detection efficiency, the events with at least one $K^+(K^-)$ are selected for further analysis. Thus, the candidate events are required to have three or four charged tracks. A one-constraint (1C) kinematic fit is subsequently performed under the hypothesis of $\psi(3686) \rightarrow p\bar{p}K^+K^-$, where K^+ or K^- is treated as a missing particle with the nominal mass of a kaon. For the events with both kaons detected, two 1C kinematic fits are performed assuming a missing K^+ or K^- . The one with the least χ_{1C}^2 is retained. To suppress background events, the χ_{1C}^2 is required to be less than

10.

The potential backgrounds are investigated using the inclusive $\psi(3686)$ MC sample. Besides the irreducible backgrounds from the non-resonant decay $\psi(3686) \rightarrow p\bar{p}K^+K^-$, the reducible backgrounds are dominated by the processes involving $\Lambda(\bar{\Lambda})$ intermediate states. To suppress the above backgrounds, all other charged tracks except for the selected proton, antiproton and kaon candidates are assumed to be pions, and events are excluded if any combination of $p\pi^-$ or $\bar{p}\pi^+$ has an invariant mass lying in the range $|M_{p\pi^-}(\bar{p}\pi^+) - M_{\Lambda(\bar{\Lambda})}| < 3 \text{ MeV}/c^2$. There are also some background events found originating from the process $\psi(3686) \rightarrow \bar{p}K^+\Lambda(1520) + c.c.$ with $\Lambda(1520) \rightarrow pK$. A MC sample is generated to describe its shape, and the number of background events of $\psi(3686) \rightarrow \bar{p}K^+\Lambda(1520)$ is expected to be 40 ± 21 , which is estimated by a fit to the measured pK^- invariant-mass spectrum. The signal shape of the $\Lambda(1520) \rightarrow pK$ is modeled with a Breit Wigner (BW) function, and the background is described with a second-order Chebychev polynomial function. Only the background from the continuum process $e^+e^- \rightarrow p\bar{p}\phi$ was found to have a peaking structure underneath the ϕ -signal region. This contribution from this background is studied using the off-resonance samples taken at $\sqrt{s} = 3.773 \text{ GeV}$, and its absolute magnitude is determined according to the formula $N = N_{survive} \cdot \frac{\mathcal{L}_{\psi(3686)}}{\mathcal{L}_{3773}} \cdot \frac{\sigma_{\psi(3686)}}{\sigma_{3773}} \cdot \frac{\varepsilon_{\psi(3686)}}{\varepsilon_{3773}}$, where $N_{survive}$ is the number of events which remained in the off-resonance samples after applying the same event selections that are used to identify $\psi(3686) \rightarrow p\bar{p}\phi$. \mathcal{L} , σ and ε refer to the integrated luminosities ($\mathcal{L}_{\psi(3686)} = 668.55 \text{ pb}^{-1}$ [17], $\mathcal{L}_{3773} = 2931.8 \text{ pb}^{-1}$ [28]), the cross sections and the detection efficiencies of the data samples taken at the two corresponding center-of-mass energies, respectively. Figure 1 shows the K^+K^- invariant-mass spectrum after applying all the selection criteria mentioned above. Note that a clear signal corresponding to the decay $\phi \rightarrow K^+K^-$ is visible in the spectrum. Figure 2 shows the Dalitz plot of $\psi(3686) \rightarrow p\bar{p}\phi$ for the events with a K^+K^- invariant-mass that falls within the ϕ -mass region ($1.005 \text{ GeV}/c^2 < M_{K^+K^-} < 1.035 \text{ GeV}/c^2$). The data show no evident resonance structures. Figure 3 shows its projections on the $p\phi$ and $\bar{p}\phi$ invariant-mass distributions. These distributions show that the data are well described by a phase-space distribution of the signal channel together with the continuum background and non-peaking background.

B. Measurement of $\mathcal{B}(\psi(3686) \rightarrow p\bar{p}\phi)$

The ϕ -signal yields are obtained from an extended unbinned maximum-likelihood fit to the K^+K^- invariant-mass spectrum in the range of $[0.985, 1.115] \text{ GeV}/c^2$. In the fit, the ϕ signal component is modeled by the MC-simulated signal shape convoluted with a Gaussian function to account for the difference in the mass resolution between data and MC simulation. The MC sample,

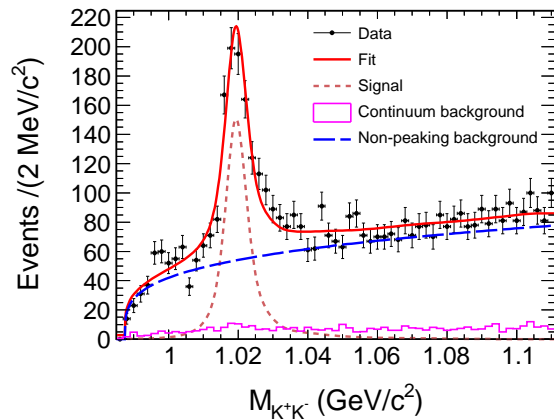


FIG. 1. Fit to K^+K^- invariant-mass spectrum. The dots with error bars represent the data, the red solid line is the global fit result, the brown short dashed line represent the signal shape, the pink histogram is the contribution of the continuum background, and the blue long dashed line reflects the non-peaking background.

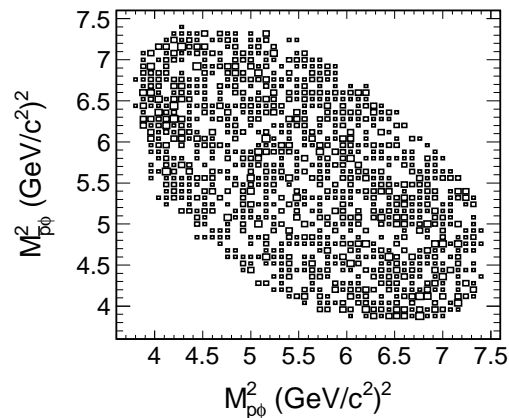


FIG. 2. Dalitz plot for $\psi(3686) \rightarrow p\bar{p}\phi$ for the events with a K^+K^- invariant mass that falls within the ϕ -mass region ($1.005 \text{ GeV}/c^2 < M_{K^+K^-} < 1.035 \text{ GeV}/c^2$).

$\psi(3686) \rightarrow p\bar{p}\phi$, is generated according to a phase-space assumption. The background contribution from the continuum process $e^+e^- \rightarrow p\bar{p}\phi$ is obtained as discussed above and its shape and yield are fixed in the fit. The other background events are parameterized by a modified ARGUS function [29]. The parameters of the Gaussian function and the ARGUS function are left free in the fit. The fit, shown in Fig. 1, yields $N_{obs} = 753 \pm 47$ signal events. The statistical significance is found to be 21σ , which is determined from the change in $-2 \ln L$ in the fits of mass spectrum with and without assuming the presence of a signal while considering the change in degrees of freedom of the fits.

The branching fraction of $\psi(3686) \rightarrow p\bar{p}\phi$ is calculated

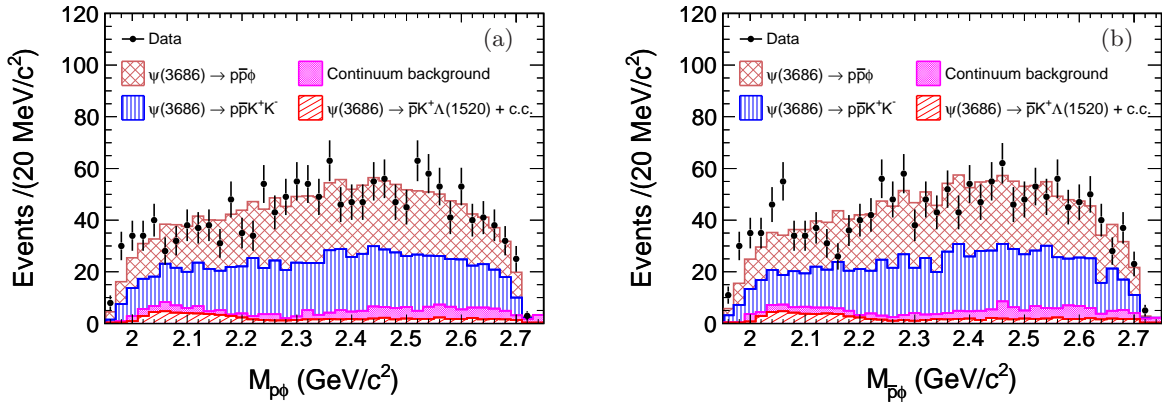


FIG. 3. The invariant-mass distribution of (a) $p\phi$ and (b) $\bar{p}\phi$. The dots with error bars denote the data; the contributions for each component are indicated as the hatched histograms.

with,

$$\begin{aligned} \mathcal{B}(\psi(3686) \rightarrow p\bar{p}\phi) \\ = \frac{N_{obs}}{N_{\psi(3686)} \times \mathcal{B}(\phi \rightarrow K^+K^-) \times \varepsilon}, \end{aligned} \quad (2)$$

where N_{obs} is the number of the observed signal events which comes from the fit. $N_{\psi(3686)}$ is the total number of $\psi(3686)$ events. The branching fraction of $\phi \rightarrow K^+K^-$, $\mathcal{B}(\phi \rightarrow K^+K^-) = (49.2 \pm 0.5)\%$, is taken from the PDG [24]. ε is the detection efficiency. To obtain a reliable detection efficiency, the MC sample of $\psi(3686) \rightarrow p\bar{p}\phi$, distributed according to a phase-space assumption, is weighted to match the distribution of the background-subtracted data with the mass distribution of $p\bar{p}$, and the average detection efficiency is determined to be 56.4%. The branching fraction, $\mathcal{B}(\psi(3686) \rightarrow p\bar{p}\phi)$, is measured to be $(6.06 \pm 0.38 \pm 0.48) \times 10^{-6}$, where the uncertainties are the statistical and systematic uncertainty, respectively. The systematic uncertainties will be discussed in detail in the following section.

C. Systematic uncertainties

The systematic uncertainties that affect the branching-fraction measurement can be divided into two categories. The first category is given by the uncertainties in the track reconstruction, the particle identification (PID), 1C kinematic fit, and $\Lambda/\bar{\Lambda}$ veto efficiency. The other category comprises the uncertainties which originate from the fit of the mass spectrum, the weighting procedure, the cited branching fraction of the decay of the intermediate state, and the total number of $\psi(3686)$ events.

The difference in the efficiencies of the track reconstruction for p/\bar{p} between MC and data is studied using a clean sample of $J/\psi \rightarrow p\bar{p}\pi^+\pi^-$ and found to be less than 1.0% per track. For the K^\pm , the systematic uncertainty is studied using a clean control sample of $J/\psi \rightarrow K_S^0 K^\pm \pi^\mp$. 1.0% per tracking is taken as the systematic uncertainty for the tracking efficiency [30].

The PID efficiency of p/\bar{p} is also studied from the same data sample of $J/\psi \rightarrow p\bar{p}\pi^+\pi^-$. The results indicate that the p/\bar{p} PID efficiency for data agrees with the MC simulation within 1%. The PID efficiency for the kaon is measured in the clean channel $J/\psi \rightarrow K^+K^-\eta$. It is found that the difference between the PID efficiency of data and MC is less than 1% for each kaon. In this analysis, three charged tracks are required to be identified as a proton, an anti-proton and a kaon. Hence, 3% is taken as the systematic uncertainty associated with the PID.

With a clean control sample of $\psi(3686) \rightarrow pK^-\bar{\Lambda} + c.c.$, the systematic uncertainty of the 1C kinematic fit is estimated to be 3.4% by calculating the difference of ratio of signal yields with χ_{1C}^2 cut and without 1C kinematic fit between MC simulation and data.

To veto the $\Lambda/\bar{\Lambda}$ background events, $|M_{p\pi^-/\bar{p}\pi^+} - M_{\Lambda/\bar{\Lambda}}| > 3 \text{ MeV}/c^2$ is required. An alternative choice of $|M_{p\pi^-/\bar{p}\pi^+} - M_{\Lambda/\bar{\Lambda}}| > 10 \text{ MeV}/c^2$ is used to remeasure the branching fraction. A difference of 1.1% is found and taken as the corresponding systematic uncertainty.

The ϕ -signal yields are obtained by fitting the K^+K^- invariant-mass spectrum. Systematic uncertainties related to the fit have been estimated by using different signal and background shapes, alternative fit ranges, and by taking into consideration an additional resonant structure. To estimate the uncertainty from the modeling of the ϕ -signal shape, an alternative fit with an acceptance-corrected BW function to describe the ϕ -signal has been performed. To estimate the uncertainty due to the background shape, a function of $f(M) = (M - M_a)^c (M_b - M)^d$ is used instead of the modified ARGUS function, where, M_a and M_b are the lower and upper edges of the mass distribution, respectively, and c and d are free parameters. In the K^+K^- invariant-mass distribution, we observed a small bump around $1 \text{ GeV}/c^2$. Although this structure might be due to statistical fluctuations, we considered the possibility of an additional resonance. We, therefore, fitted the distribution with an extra BW function convolved with a Gaussian function. The change of signal

yield in the different fit is taken as the corresponding systematic uncertainty. The quadratic sum of the four individual uncertainties is taken as the systematic uncertainty related with the mass spectrum fit, and it is found to be 5.5%.

To obtain a reliable detection efficiency, the MC sample modeled using a phase-space distribution is weighted to match the distribution of the background-subtracted data. To consider the effect on the statistical fluctuations of the signal yield in the data, a set of toy-MC samples are used to estimate the detection efficiencies. With the reweighting, a maximum deviation in detection efficiencies of 1.0% is found and quoted as the corresponding systematic uncertainty.

The branching fraction uncertainty of the intermediate decay $\phi \rightarrow K^+K^-$, 1.0%, is taken from the PDG and the uncertainty of the number of $\psi(3686)$ events is 0.6% [17].

In Table I, a summary is shown of all contributions to the systematic uncertainties on the branching fraction measurements. The total systematic uncertainty is given by the quadratic sum of the individual contributions, assuming all sources to be independent.

TABLE I. Sources of relative systematic uncertainties and their contributions to the branching fractions and upper limits (in %).

| Sources | $p\bar{p}\phi$ | $X(p\bar{p})\phi$ |
|--|----------------|-------------------|
| MDC tracking | 3.0 | 3.0 |
| PID efficiency | 3.0 | 3.0 |
| 1C kinematic fit | 3.4 | 3.4 |
| $\Lambda(\bar{\Lambda})$ veto | 1.1 | 1.1 |
| Mass spectrum fit | 5.5 | — |
| Weighting procedure | 1.0 | — |
| $\mathcal{B}(\phi \rightarrow K^+K^-)$ | 1.0 | 1.0 |
| Number of $\phi(3686)$ events | 0.6 | 0.6 |
| Total | 8.0 | 5.7 |

D. Upper limit of $p\bar{p}$ mass threshold enhancement

Figure 4 depicts the $p\bar{p}$ invariant-mass distribution for the events with a K^+K^- invariant mass that falls within the ϕ mass region ($1.005 \text{ GeV}/c^2 < M_{K^+K^-} < 1.035 \text{ GeV}/c^2$), where no evident enhancement near the $p\bar{p}$ -mass threshold is visible. It is found that the events from the phase-space process together with other background components provide a good description of the data, which is shown in Fig. 4. Therefore, an upper limit for the $X(p\bar{p})$ production rate can be measured. For $J/\psi \rightarrow p\bar{p}\phi$, we divide $p\bar{p}$ invariant-mass spectrum into 9 bins in the region of $[1.876, 2.056] \text{ GeV}/c^2$. With the same procedure as described above, the number of the ϕ events in each bin can be obtained by fitting to the corresponding K^+K^- -mass spectrum. Subsequently, the non- ϕ -background-subtracted $M_{p\bar{p}}$ distribution is obtained as shown in Fig. 5, where the errors are statistical only, and m_p is the nominal mass of proton [24].

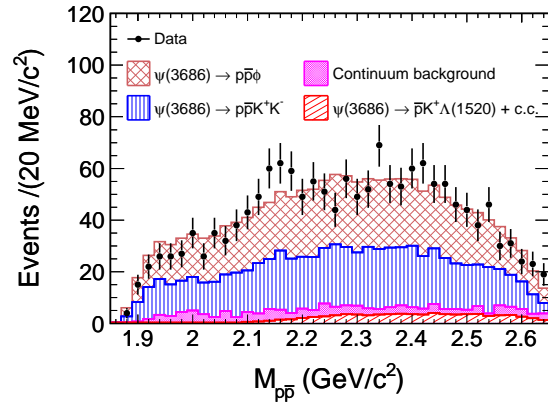


FIG. 4. The $p\bar{p}$ invariant-mass distribution. The dots with error bars denote the data; the contributions for each component are displayed as the hatched histograms.

The spin (J) and parity (P) of $X(p\bar{p})$ have been determined by an amplitude analysis of $J/\psi \rightarrow \gamma p\bar{p}$ decay and resulted in $J^{PC} = 0^{-+}$ [4]. In our analysis, we parametrize the $X(p\bar{p})$ signal by an efficiency-weighted S -wave BW function,

$$BW(M) \simeq \frac{f_{FSI} \times q^{2L+1} \kappa^3}{(M^2 - M_0^2)^2 + M_0^2 \Gamma_0^2} \times \varepsilon_{rec}(M), \quad (3)$$

where M is the $p\bar{p}$ invariant mass, the parameter f_{FSI} accounts for the effect of the FSI, q is the momentum of the proton in the $p\bar{p}$ rest frame, κ is the momentum of ϕ in the $\psi(3686)$ rest frame, $L = 0$ is the relative orbital angular momentum of the $p\bar{p}$ system, M_0 and Γ_0 are the mass and width of $X(p\bar{p})$, respectively, which are fixed to those in Ref. [4]. $\varepsilon_{rec}(M)$ is the mass-dependent detection efficiency which is obtained from MC simulations of $\psi(3686) \rightarrow X(p\bar{p})\phi \rightarrow p\bar{p}\phi$. We ignore possible interference effects of the $X(p\bar{p})$ resonance with non-resonant background contributions.

To determine the upper limit on the size of the $p\bar{p}$ enhancement, a series of binned least- χ^2 fits are performed to the background-subtracted $p\bar{p}$ -mass spectrum with the expected signal. Fit-related uncertainties are included by considering the following three aspects: (a) the $X(p\bar{p})$ signal is described by excluding the FSI factor with $f_{FSI} = 1$ or taking into account the Jülich FSI value as described in Ref. [13]; (b) the non-resonant background is represented by the shape obtained from the $\psi(3686) \rightarrow p\bar{p}\phi$ MC simulation or parameterized by a function of $f(\delta) = N(\delta^{1/2} + a_1\delta^{3/2} + a_2\delta^{5/2})$ ($\delta = M_{p\bar{p}} - 2m_p$, a_1 and a_2 are free parameters); and (c) the fit is performed in the range of $[0.00, 0.18] \text{ GeV}/c^2$ or $[0.00, 0.20] \text{ GeV}/c^2$. Therefore, there are eight alternative fit scenarios. In the variations, the fit taking into account the FSI, with the background parameterized by the function of $f(\delta)$ in the range $[0.0, 0.18] \text{ GeV}/c^2$, gives the maximum number of $X(p\bar{p})$ candidates, 20.6, at the 90% C.L.. The corresponding fitting plot is shown in Fig. 5, and the upper

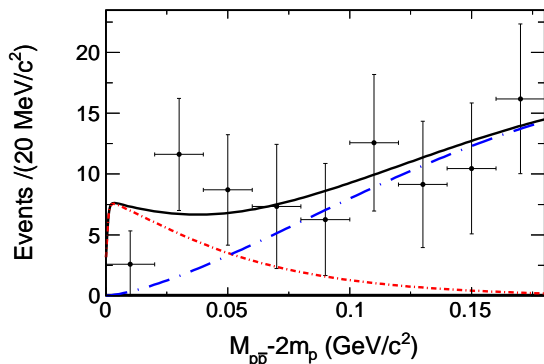


FIG. 5. Distributions of $M_{p\bar{p}} - 2m_p$ and fit result corresponding to the upper limit on the branching fraction at the 90% C.L.. The dots with error bars represent the data, the black solid line is the global fit result, the red dashed-dotted line is the $X(p\bar{p})$ signal, and the blue long-dashed-dotted line denotes the non-resonant background.

limit on the branching fraction is determined by,

$$\mathcal{B}(\psi(3686) \rightarrow X(p\bar{p})\phi \rightarrow p\bar{p}\phi) < \frac{N^{UL}}{N_{\psi(3686)} \times \mathcal{B}(\phi \rightarrow K^+K^-) \times \varepsilon}, \quad (4)$$

where N^{UL} is the maximum number of $X(p\bar{p})$ events. To be conservative, the multiplicative uncertainties listed in Table I are considered by convoluting the normalised χ^2 distribution with a Gaussian function. The detection efficiency, ε , is obtained from MC simulations, and is determined to be 58.9%. The upper limit on the branching fraction of $\psi(3686) \rightarrow X(p\bar{p})\phi \rightarrow p\bar{p}\phi$ at the 90% C.L. is calculated to be 1.82×10^{-7} .

IV. SUMMARY

Using a sample of 4.48×10^8 $\psi(3686)$ events accumulated with the BESIII detector, we present a study of the decay $\psi(3686) \rightarrow p\bar{p}\phi$. The branching fraction of $\psi(3686) \rightarrow p\bar{p}\phi$ is measured for the first time and it is found to be $[6.06 \pm 0.38(\text{stat.}) \pm 0.48(\text{syst.})] \times 10^{-6}$. With

the previously published branching-fraction measurement of $J/\psi \rightarrow p\bar{p}\phi$ [14], the ratio $Q = \frac{\mathcal{B}(\psi(3686) \rightarrow p\bar{p}\phi)}{\mathcal{B}(J/\psi \rightarrow p\bar{p}\phi)}$ is determined to be $(11.6 \pm 0.7 \pm 1.2)\%$. With the same approach as given in Ref. [32], we also present the ratio by taking the phase spaces of $J/\psi/\psi(3686) \rightarrow p\bar{p}\phi$ into account. The phase-space ratio of them is determined to be $\Omega_{\psi(3686) \rightarrow p\bar{p}\phi} / \Omega_{J/\psi \rightarrow p\bar{p}\phi} = 11.9$. By taking this into consideration, the Q value becomes $(0.97 \pm 0.06 \pm 0.10)\%$, which indicates that the ‘12% rule’ is violated significantly. No evidence for an enhancement near the $p\bar{p}$ -mass threshold is found and the upper limit on the branching fraction of $\psi(3686) \rightarrow X(p\bar{p})\phi \rightarrow p\bar{p}\phi$ is determined to be 1.82×10^{-7} at the 90% C.L..

ACKNOWLEDGMENTS

The BESIII collaboration thanks the staff of BEPCII and the IHEP computing center for their strong support. This work is supported in part by National Key Basic Research Program of China under Contract No. 2015CB856700; National Natural Science Foundation of China (NSFC) under Contracts Nos. 11335008, 11425524, 11625523, 11635010, 11735014, 11565006; the Chinese Academy of Sciences (CAS) Large-Scale Scientific Facility Program; the CAS Center for Excellence in Particle Physics (CCEPP); Joint Large-Scale Scientific Facility Funds of the NSFC and CAS under Contracts Nos. U1332201, U1532257, U1532258, U1732263; CAS Key Research Program of Frontier Sciences under Contracts Nos. QYZDJ-SSW-SLH003, QYZDJ-SSW-SLH040; 100 Talents Program of CAS; INPAC and Shanghai Key Laboratory for Particle Physics and Cosmology; German Research Foundation DFG under Contract No. Collaborative Research Center CRC 1044; Istituto Nazionale di Fisica Nucleare, Italy; Koninklijke Nederlandse Akademie van Wetenschappen (KNAW) under Contract No. 530-4CDP03; Ministry of Development of Turkey under Contract No. DPT2006K-120470; National Science and Technology fund; The Swedish Research Council; U. S. Department of Energy under Contracts Nos. DE-FG02-05ER41374, DE-SC-0010118, DE-SC-0012069; University of Groningen (RuG) and the Helmholtzzentrum fuer Schwerionenforschung GmbH (GSI), Darmstadt

[1] J. Z. Bai *et al.* (BES Collaboration), Phys. Rev. Lett. **91**, 022001 (2003).
 [2] J. P. Alexander *et al.* (CLEO Collaboration), Phys. Rev. D **82**, 092002 (2010).
 [3] M. Ablikim *et al.* (BESIII Collaboration), Chin. Phys. C **34**, 421 (2010).
 [4] M. Ablikim *et al.* (BESIII Collaboration), Phys. Rev. Lett. **108**, 112003 (2012).

[5] S. B. Athar *et al.* (CLEO Collaboration), Phys. Rev. D **73**, 032001 (2006).
 [6] M. Ablikim *et al.* (BES Collaboration), Eur. Phys. J. C **53**, 15 (2008).
 [7] M. Ablikim *et al.* (BESIII Collaboration), Phys. Rev. Lett. **106**, 072002 (2011).
 [8] M. Ablikim *et al.* (BESII Collaboration), Phys. Rev. Lett. **95**, 262001 (2005).

- [9] A. Datta and P. J. O'Donnell, Phys. Lett. B **567**, 273 (2003).
- [10] M. L. Yan, S. Li, B. Wu and B. Q. Ma, Phys. Rev. D **72**, 034027 (2005).
- [11] M. Abud, F. Buccella, and F. Tramontano, Phys. Rev. D **81**, 074018 (2010).
- [12] B. S. Zou and H. C. Chiang, Phys. Rev. D **69**, 034004 (2004).
- [13] A. Sibirtsev, J. Haidenbauer, S. Krewald, U. Meissner, and A. W. Thomas, Phys. Rev. D **71**, 054010 (2005).
- [14] M. Ablikim *et al.* (BESIII Collaboration), Phys. Rev. D **93**, 052010 (2016).
- [15] M. Ablikim *et al.* (BESIII Collaboration), Phys. Rev. D **67**, 052002 (2003).
- [16] R. A. Briere *et al.* (CLEO Collaboration), Phys. Rev. Lett. **95**, 062001 (2005).
- [17] M. Ablikim *et al.* (BESIII Collaboration), Chin. Phys. C **42**, 023001 (2018).
- [18] T. Appelquist and H. D. Politzer, Phys. Rev. Lett. **34**, 43 (1975).
- [19] M. Ablikim *et al.* (BESIII Collaboration), Nucl. Instrum. Methods Phys. Res., Sect. A **614**, 345 (2010).
- [20] C. H. Yu *et al.*, Proceedings of IPAC2016, Busan, Korea, 2016, doi:10.18429/JACoW-IPAC2016-TUYA01.
- [21] S. Agostinelli *et al.* (GEANT4 Collaboration), Nucl. Instrum. Methods Phys. Res., Sect. A **506**, 250 (2003).
- [22] S. Jadach, B. F. L. Ward and Z. Was, Phys. Rev. D **63**, 113009 (2001); Comput. Phys. Commun. **130**, 260 (2000).
- [23] D. J. Lange, Nucl. Instrum. Methods Phys. Res., Sect. A **462**, 152 (2001); R. G. Ping, Chin. Phys. C **32**, 599 (2008).
- [24] M. Tanabashi *et al.* (Particle Data Group), Phys. Rev. D **98**, 030001 (2018).
- [25] J. C. Chen, G. S. Huang, X. R. Qi, D. H. Zhang and Y. S. Zhu, Phys. Rev. D **62**, 034003 (2000); R. L. Yang, R. G. Ping and H. Chen, Chin. Phys. Lett. **31**, 061301 (2014).
- [26] E. Richter-Was, Phys. Lett. B **303**, 163 (1993).
- [27] W. D. Li, H. M. Liu *et al.*, in proceeding of CHEP06, Mumbai, India, 2006 edited by Sunanda Banerjee (Tata Institute of Fundamental Reserach, Mumbai, (2006).
- [28] M. Ablikim *et al.* (BESIII Collaboration), Phys. Lett. B **753**, 629 (2016).
- [29] H. Albrecht *et al.* (ARGUS Collaboration), Phys. Lett. B **340**, 217 (1994).
- [30] M. Ablikim *et al.* (BESIII Collaboration), Phys. Rev. D **83**, 112005 (2011).
- [31] M. Ablikim *et al.* (BESIII Collaboration), Phys. Rev. D **85**, 092012 (2012).
- [32] M. Ablikim *et al.* [BESIII Collaboration], Phys. Rev. D **99**, 032006 (2019).